

Hybrid Algorithm Based on Hyper Spectral Noise Removal for Satellite Image

N. Hema Rajini¹

¹Associate Professor, Department of Computer Science and Engineering, Alagappa Chettiar Government College of Engineering and Technology, Karaikudi – 630003, Tamil Nadu (State), India.

Abstract

Usually the image obtained from a sensor is blurred by noise. Such noises are identified and eliminated by the procedure called denoising. The cross breed (Hybrid) algorithm is a popular technique that has been utilized recently. The Discrete Cosine Transformation (DCT) and Discrete Wave Transformation (DWT) are the generally utilized transform in which discrete cosine transformation requires less energy and computation resource and discrete wavelet transformation has multiple transformations. This Hybrid Algorithm combines the twin benefits of both the transformation and thus eliminates the negative contour and blocks the traces completely. The effectiveness of the proposed hybrid Algorithm is verified with different pictures by finding the average Squared Blunder, PSNR, Variance, architectural resemblance Index and average architectural resemblance Index.

Keywords: Denoising, MSE, MSSIM, PSNR, SSI, Squared Blunder

Received on 18 February 2020, accepted on 25 March 2020, published on 26 March 2020

Copyright © 2020 N. Hema Rajini *et al.*, licensed to EAI. This is an open access article distributed under the terms of the Creative Commons Attribution licence (<http://creativecommons.org/licenses/by/3.0/>), which permits unlimited use, distribution and reproduction in any medium so long as the original work is properly cited.

doi: 10.4108/eai.13-7-2018.163843

*Corresponding author. Email: auhemasmith@yahoo.co.in

1. Introduction

The clamors less pictures are essential in satellite application. MPEG-4 is the cutting edge visual coding calibers that give higher flexibility while evaluating mixed media for a visual item based application and redesign the visual force at least bit rate and can be utilized to get and estimate each item [Schafer, R.,]. The

discretionary formed visual item should save its size and surface. The current strategies incorporate square shaped picture and recordings and programming like DCT and DWT. In customary strategies, the bouncing box fixes the subjectively pictures, in the outside side of the item pixel location esteems are cushioned in the inner side, the object pixels are coded and cushioned in the bouncing box together, may be wasteful [3]-[7]. The issue of evacuating the commotion in visual items without deteriorating its properties (edges, surfaces,

hues, differentiate, and so forth) has been explored throughout the previous two decades and numerous different kinds of denoising systems have been created. The complete change based commotion expelling technique created by had a lot of impact in picture and motivate an enormous amount of definitions for evacuating the commotion of a picture. The Non Local Mean (NLM) calculation figures out in [Mitra, S.K.] to accurately expel a large portion of the clamors but, they cannot appropriately recoup a portion of the picture subtleties. These techniques additionally manage added substance Gaussian commotion, though for some pictures the clamor model is obscure, such that there is plenty of opportunity available to get better performance [Zhijun, F.,]

In this paper the Hybrid Algorithm is applied to denoise different satellite pictures. The present Transform utilized for denoising the pictures are discussed in section II. The Hybrid algorithm intended for lessening arty-craft is depicted in section III. The output of the different calculations and correlations with other coding strategies for various pictures are reported in section IV. The conclusion of the paper is presented in section V.

2. Literature Review

For mobile communication and broadband services, MPEG-4 was utilized for realizing interactive multimedia communication with a data rate of 5 Kbps-15 Mbps. A hybrid ICT compressor provided video compression. To efficiently identify the motions in all environments and random images of objects were coded by several tools [Schafer, R.,]. In [Hsiang, S.T.,] an efficient application specific EZB coder with context modelling and node tree splitting was proposed to improve the compression efficiency of existing coder. There exists strong interdependency with the modelling and splitting. To minimize the prediction mistake of the frames, a hybrid transformation with inter and intra frames were coded by DCT and DWT [Ezhilarasan, M.,]. This proposal selects the required frames from the intra frames. An object oriented hybrid image coding algorithm was proposed and is more efficient than SPIHT coding. This new scattering of the wave coefficient diminishes computational unpredictability. In the event of lower bit rate picture programming, one course of action go in the wavelet field was applied. The benefit of OB-HIC lies in the DWT maps with little coefficients in all sub-band picture information. A hybrid picture programming [Mohammed, U.S.,] which integrates embedded zero tree DWT with DCT block and found to be more efficient than EZW method since one scale wave rotting where one leading pass and one substitute pass were considered. The performance of the proposed method was greater than the JPEG consecutive coding and block influence

with the recent method has minimum effect than with the JPEG consecutive coding method.

3. Existing Transforms for Denoising

Discrete Cosine Transformation (DCT) Source information focuses are demonstrated by DCT as a cos work with different wavering recurrence and magnitude. The two principle kinds of DCT plans are: discrete 1-D cos change and discrete 2-D cos change. Since a picture is converted into two 2 dimensional network, 2-D discrete cosine change is utilized. The 2-dimensional DCT for a input sequence of size x is described [Qi, H., Huang, Q.,] as

$$D_{DCT}(i, j) = \frac{1}{\sqrt{2N}} B(i)B(j) \sum_{x=0}^{N-1} \sum_{y=0}^{N-1} M(x, y) \cos \left[\frac{2x+1}{2N} i\pi \right] \cos \left[\frac{2x+1}{2N} j\pi \right] \quad (1)$$

Where, $B(u) = \begin{cases} \frac{1}{2} & \text{if } u=0 \\ 1 & \text{if } u>0 \end{cases}$
 x, y is the input data size $M(x, y)$

In DCT, every single data were obliging in a small number at minimum recurrence coefficients which are effectively influenced by commotion. The coefficient with low recurrence is called as DC segments and other coefficients are identified AC parts. Utilizing 8×8 quantization table, the DCT coefficients are quantized similar to the JPGE standard. The condition for 2-D opposite DCT change is given below (Figure 1).

$$D_{IDCT}(i, j) = \frac{1}{\sqrt{2N}} \sum_{x=0}^{N-1} \sum_{y=0}^{N-1} B(i)B(j) Ddequant(i, j) \cos \left[\frac{2x+1}{2N} i\pi \right] \cos \left[\frac{2x+1}{2N} j\pi \right] \quad (2)$$

Where, $B(u) = \begin{cases} \frac{1}{2} & \text{if } u=0 \\ 1 & \text{if } u>0 \end{cases}$

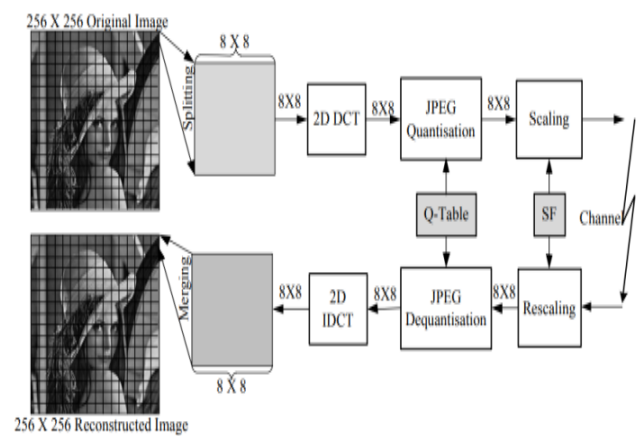


Figure 1. Construction of 2D-DCT

The several constraints of DCT are artefact and negative Contour. The mutilation like artefact block happens because of high pressure rate similar to huge pixel block. The bogus contour occurs because of easily reviewed territory of visual items that are misshaped and shown up as a shape map for pictures . The overwhelming quantization of the change coefficients is the main reason for false contouring effect.

Discrete Wavelet Transformation (DWT) This transformation shows the visual data as the aggregate of wavelet, and called as wavelet with different area and various scales [Pearlman, W]. The high pass (details) coefficient and low pass (inexact) coefficients are the featured information. For moving the information, channel sets with low pass and high pass is used adequately. For this, channel kernel is $\begin{bmatrix} 1 & 1 \\ 1 & -1 \end{bmatrix}$. By 2 factor, yield of high and low pass channels are down examined. This procedure is 1-D DWT and the schematic is shown in **Figure 2**.

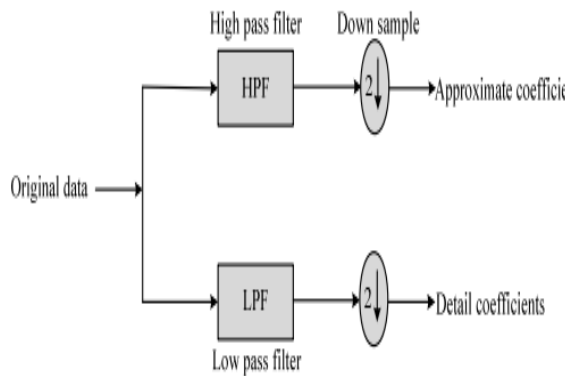


Figure 2. Block diagram of 1D forward DWT

In two dimensional DWT, low and high pass channel source information is sent in different direction line and list. The output is down sampled by 2 in all the direction. The overall step is given in **Figure 3**. The yield is received as 4 coefficients LL, LH, HL and HH. [Fan C., and Su, G]. Line transforms make the first alphabet and list transforms make the next alphabet. The word L indicates low pass signal and H represents high pass signal. In line, low pass signal is depicted as LH signal and in the list high pass signal is marked as HH. LH signal composed of parallel component, and HL and HH are the vertical and diagonal components.

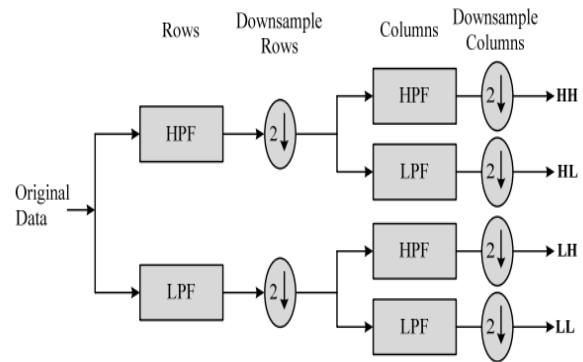


Figure 3. Block diagram of 2D forward DWT

As given in **Figure 4**, when DWT is reconstructed, source information is received without integrating LL coefficients for level with several dissimilar resolutions [38]. To reanalyze the yield, minimized data is up sampled by 2. Then the data was directed via same high pass and low pass channels in line and list. The total recreation procedure is provided in **Figure 5**.

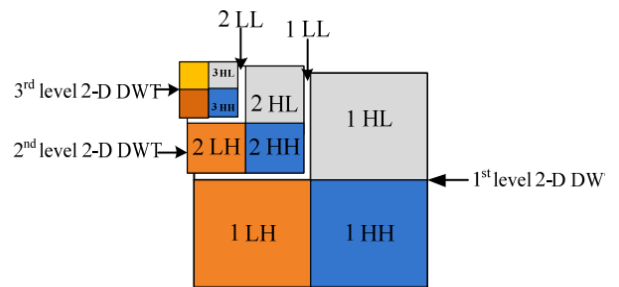


Figure 4. Multilevel Forward DWT

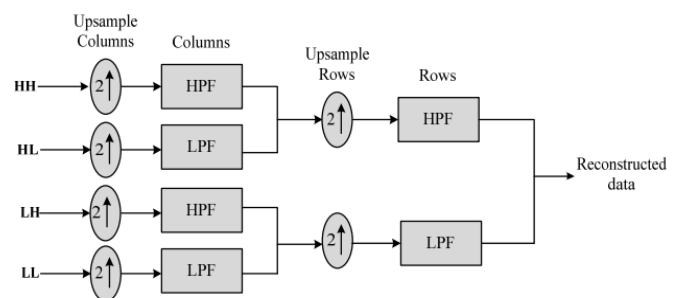


Figure 5. Block diagram of 2D Inverse DWT

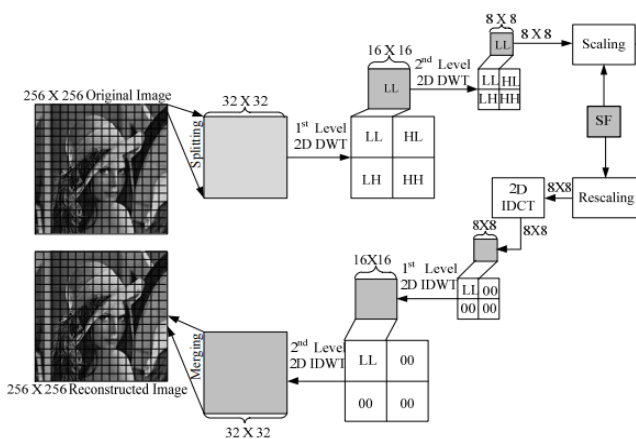


Figure 6. Block diagram of DWT Decomposition

This process continues for other levels. The coefficients are split by constant scaling factor to get the needed pressure proportion. Finally, the data is reconstructed by rescaling and padded with zero and sent to the wavelet filter. **Figure 6** represents overall process of 2D DWT compression and reconstruction.

4. Proposed Hybrid Algorithms

The DCT and DWT were used for denoising of images. DCT consumes less energy and requires few computation resources, while DWT has multiple resolution transforms. The proposed (Hybrid) Algorithm enjoys the advantages of both (DCT & DWT) the algorithm and hence reduces the negative contour and blocks the artefact efficiently.

The algorithm is developed such that the sub-samples are performed in DCT whereas the primary blocks are performed by DWT in Hybrid DWT-DCT as given in **Figure 7 & 8**.

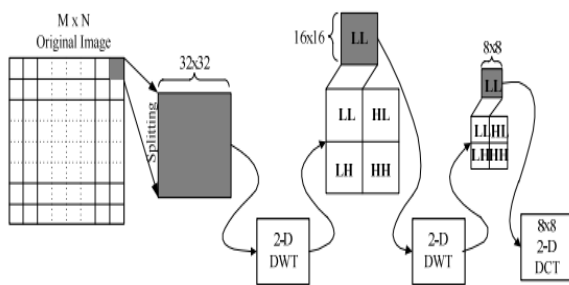


Figure 7. Schematic form of Hybrid DWT-DCT Algorithm

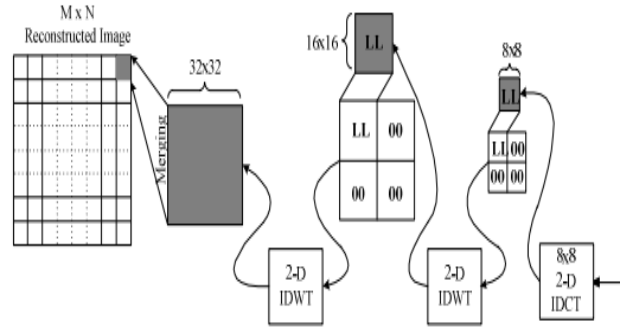


Figure 8. Representation of Inverse Hybrid DWT-DCT Algorithm

Algorithm for Hybrid DWT-DCT:

Depending on DCT and DWT algorithm, the sub-sampling strategy discussed overhead, the steps involved in Hybrid algorithm for satellite images are given below.

- 1) Consider the input satellite image.
- 2) Estimate the noise in the image.
- 3) Process the 2D DWT with suitable sub sampling method.
- 4) Select the coefficients of wavelet that need to be processed by 2D DWT and got the wavelet coefficients for next level low pass.
- 5) Process the 2D DCT with the received low pass coefficients.
- 6) Do the 2D opposite DCT and successively perform 2-D Inverse DWT for two times to reconstruct the denoised image.

Similar to this, the subsamples are deal with DWT whereas the primary blocks are operated by DCT in Hybrid DCT-DWT which is depicted in **Figure 9 & 10**.

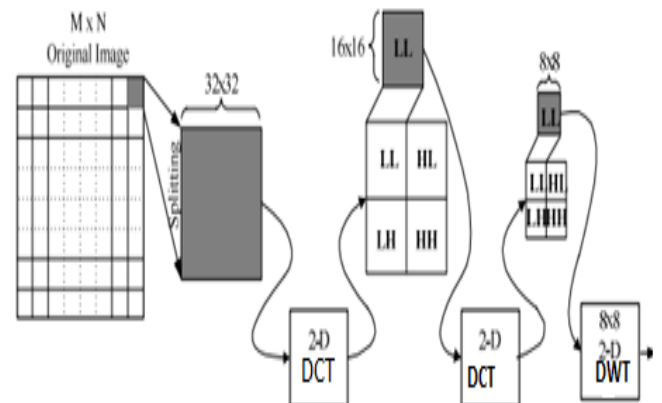


Figure 9. Hybrid DWT-DCT Algorithm

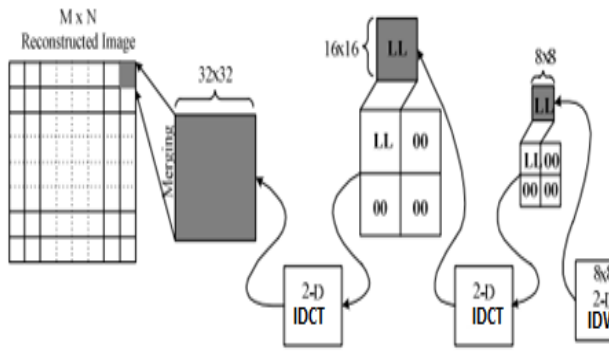


Figure 10. Inverse Hybrid DWT-DCT Algorithm

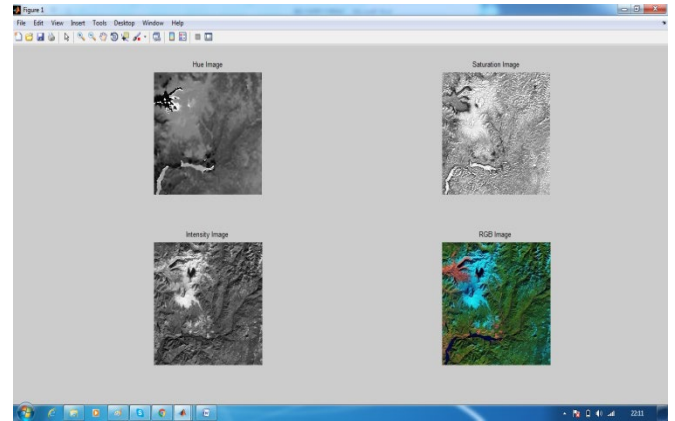


Figure 12. Satellite picture - 2

5. Results and Discussion

The Algorithm is programmed and verified in MATLAB. The satellite pictures (**Figure 11-15**) taken to evaluate the performance are given below. The effectiveness of hybrid algorithm is contrasted with present algorithm with regards to MSE, PSNR, SSI and MSSl.

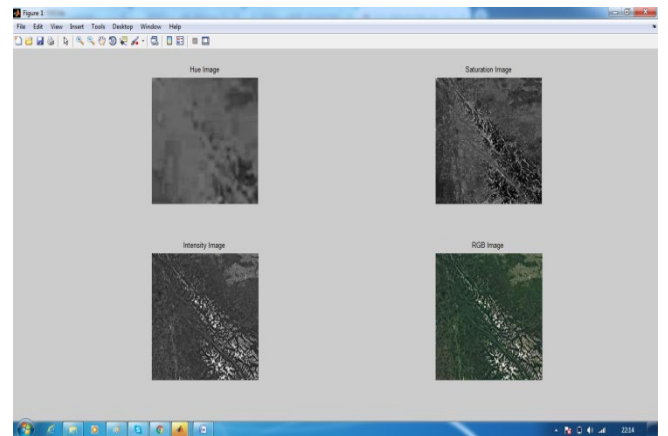


Figure 13. Satellite picture - 3

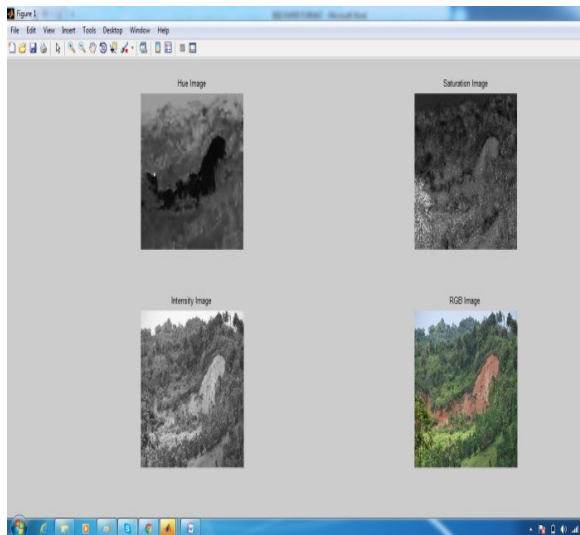


Figure 11. Satellite picture - 1

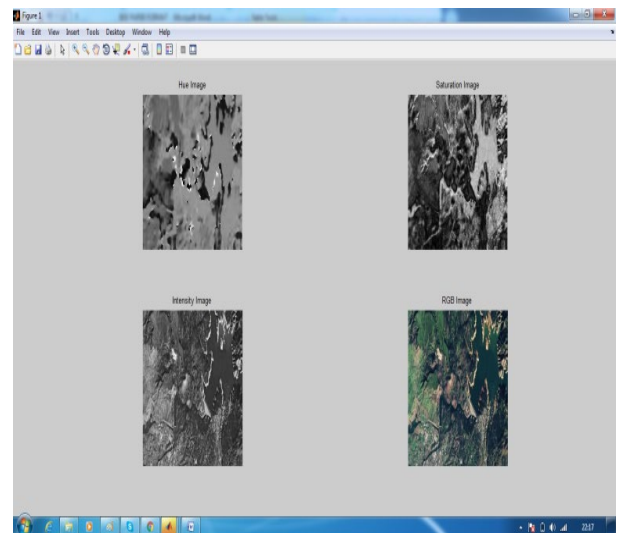


Figure 14. Satellite picture - 4

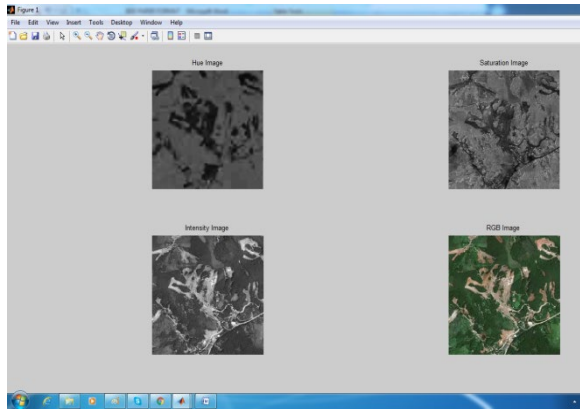


Figure 15. Satellite picture - 5

The equivalent noise estimates are measured for every filter as given in Figure 16, noises exist in the pictures.

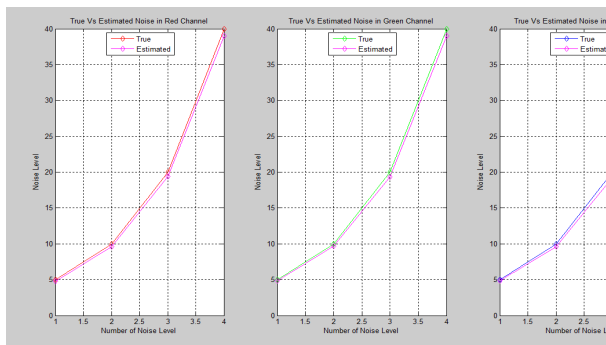


Figure 16. Noise Estimate for Test Images

The proportion of the maximum signal with corrupted noise which affects the normal peak signal to noise proportion is

$$PSNR = 20 \log_{10} \left(\frac{MAX_f}{\sqrt{MSE}} \right) \quad (3)$$

where, MSE is mean square error and said to be the average squared difference between the estimated values or the average of square of errors and is given by

$$MSE = \frac{1}{mn} \sum_0^{m-1} \sum_0^{n-1} \|f(i, j) - g(i, j)\|^2 \quad (4)$$

The PSNR should be as more as possible. The average squared blunder should be as less as possible.

The variance coefficient is a measure of corresponding variation among pictures and is given by

$$\%CV = \frac{100 \sqrt{\frac{\sum X^2 - \frac{(\sum X)^2}{N}}{N-1}}}{\bar{X}} \quad (5)$$

%CV= percentage of variance coefficient

$\sum X$ = aggregate of the assay esteems

N = quantity of assay esteems

$\sum X^2$ = aggregate of square of total values

$(\sum X)^2$ = square of the sum of all assay values

\bar{X} =AM of all assay esteems

The minimum value of the variance coefficient guarantees maximum accurate value.

The similarity estimating method between two pictures is called Structural Similarity index (SSI). It is also called as an estimation of visual object quality and is contrasted with the other visual object quality and is expressed as

$$S(x, y) = f(l(x, y), c(x, y), s(x, y)) \quad (6)$$

$$SSIM(x, y) = [l(x, y)]^\alpha \cdot [c(x, y)]^\beta \cdot [s(x, y)]^\gamma \quad (7)$$

$$SSIM(x, y) = \frac{(2\mu_x\mu_y + C_1)(2\sigma_{xy} + C_2)}{(\mu_x^2 + \mu_y^2 + C_1)(\sigma_x^2 + \sigma_y^2 + C_2)} \quad (8)$$

Structure $s(x, y)$ was compared against normalized signal $(x - \mu_x)/\sigma_x$ and $(y - \mu_y)/\sigma_y$ where the parameters α, β and γ are utilized to change the comparative parameters of three components.

The quantitative analysis of average structural similarity for high resolution picture based on window size is expressed as

$$MSSIM(X, Y) = \frac{1}{M} \sum_{j=1}^M SSIM(x_j, y_j) \quad (9)$$

The processed and reconstructed images for Hybrid DWT-DCT are shown in Figure 17.

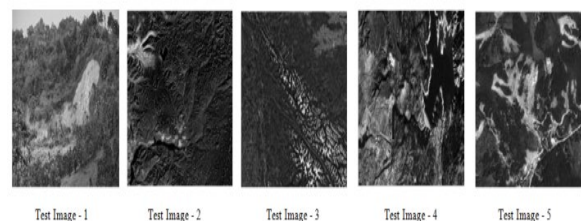


Figure 17. Reconstructed Pictures of Hybrid method

The Table 1 contains parameters involved in comparing the denoising algorithm. From the table, it is visualized that our Hybrid algorithm has the best possible attributes among all the algorithms.

Table 1. Comparison of Denoising Algorithms based on various parameters

Methods	Test Image – 1				
	MSE	PSNR	CV	SSI	MSSI
DCT	4.6172e+03	11.4869	45.4874	4.0672e-04	5.1406 e-04
DWT	751.0471	28.2299	47.0400	0.3054	0.1627
DWT-DCT	506.3219	29.8954	45.6364	0.9988	0.3229
DCT-DWT	5.1052 e+03	25.8299	60.9139	0.4682	0.0015

Test Image – 2

DCT	3.7023 e+03	12.4461	76.9491	2.6988e-04	7.9426 e-04
DWT	1.9393 e+03	27.3432	76.5332	0.2397	0.1347
DWT-DCT	569.2167	29.6713	68.9416	0.9994	0.3385
DCT-DWT	2.9860 e+03	26.7816	69.5503	0.2397	0.0988

Test Image – 3

DCT	2.8372 e+03	13.6018	54.7035	0.0047	0.0062
DWT	788.5256	28.4754	49.1566	0.4241	0.2892
DWT-DCT	483.0586	31.9986	47.3910	0.9990	0.5239
DCT-DWT	798.7914	28.1722	51.0053	0.4241	0.2882

Test Image – 4

DCT	3.7059 e+03	12.4418	69.7524	0.0074	0.0042
-----	-------------	---------	---------	--------	--------

DWT	1.0954 e+03	28.2315	57.8401	0.3804	0.2050
DWT-DCT	630.0937	30.6140	53.0960	0.9987	0.4252
DCT-DWT	1.2833 e+03	27.0931	67.0268	0.3804	0.2025

Test Image – 5

DCT	250.7565	24.1383	62.9258	0.6489	0.9334
DWT	748.4971	28.4657	60.5928	0.4329	0.2543
DWT-DCT	383.4546	31.8982	54.2012	0.9986	0.4629
DCT-DWT	839.7779	28.7878	61.2381	0.4329	0.2489

The maximum peak signal to noise ratio for Hybrid Algorithm is given in Figure 18.

Comparison of Denoising Algorithms based on PSNR

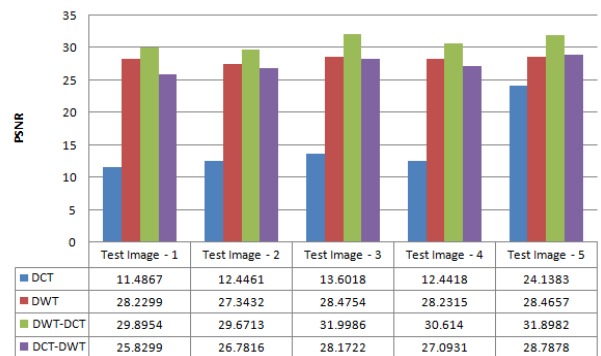


Figure 18. Comparison of Denoising Algorithms based on PSNR

The variance coefficient for Hybrid Algorithm is given in Figure 19.

Comparison of Denoising Algorithms based on Coefficient of Variance

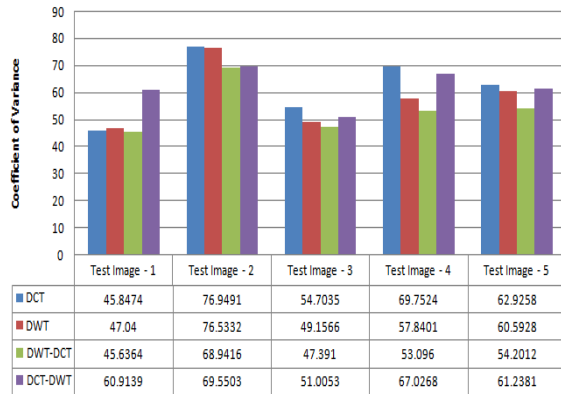


Figure 19. Comparison of Denoising Algorithm using variance coefficient

The maximum Structural Similarity Index of Hybrid Algorithm is given in Figure 20.

Comparison of Denoising Algorithms based on Structural Similarity Index

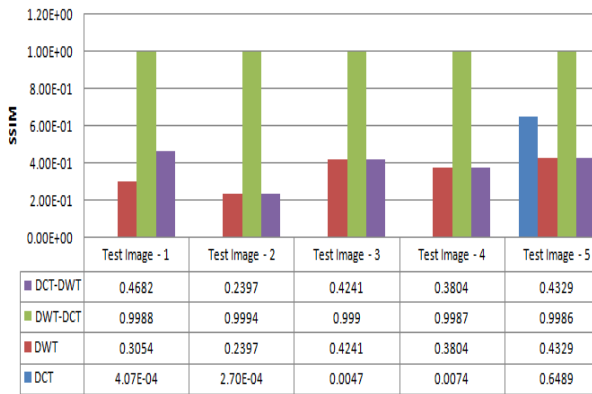


Figure 20. Comparison of Denoising Algorithms based on Structural Similarity Index

5. Conclusion

The hybrid algorithms based denoising technique is discussed in this paper. The proposed algorithms utilize the advantages of both DCT and DWT transformation effectively for denoising the images obtained from satellite. Thus, the algorithm minimizes the negative contour and blocks the artefacts efficiently. Among several denoising technique, the hybrid algorithm is a best option as its PSNR is increased by 15% with minimum MSE, Variance Coefficient, and SSI and MSSI are also

enhanced. Hence the denoised pictures prove to have low noises in the satellite image.

References

- [1] Schafer, R., and Heinrich H. (1998). A Multimedia compression standard for interactive applications and services:MPEG4. Journal of Electronics and Communication, **10**: 253-262.
- [2] Said, A., and Pearlman, W. (1997). Low-complexity waveform coding via alphabet and sample-set partitioning in visual communications and image processing, Proceedings of SPIE. pp. 25– 37.
- [3] Hsiang, S.T., and Woods, J.W. (2000). Embedded image coding using zeroblocks of subband/ wavelet coefficients and context modeling, Proceedings of ISCAS 2000 Geneva Circuits and Systems, **3**: 662–665.
- [4] Costantini, R., Bracamonte, J., Ramponi, G., Nagel, J.L., Ansorge, M., and Pellandini F. (2002) Low complexity video coder based on discrete Walsh Hadamard transform, Proceedings of European signal processing conference. pp. 1217–1220.
- [5] Ezhilarasan, M., and Thambidurai, P. (2006) A hybrid transform technique for video coding, LNCS, 4308: 503–508.
- [6] Mohammed, U.S. (2008) Highly scalable hybrid image coding scheme, Digital Signal Processing, Science Direct, (18): 364–374.
- [7] Mohammed, U.S., and Abd-elhafiez, W. M. Image coding scheme based on object extraction and hybrid transformation technique, International Journal of Engineering Science and Technology, **2**(5): 1375–1383.
- [8] Yu, T.H., and Mitra, S.K. (1997) Wavelet based hybrid image coding scheme, Proceedings of IEEE International Circuits and Systems, **1**: 377–380.
- [9] Singh, R., Kumar, V., and Verma, H. K. (2007) DWT-DCT hybrid scheme for medical image compression, Medical Engineering and Technology, **31**: pp. 109–122.
- [10] Zhijun, F., Yuanhua, Z., and Daowen, Z. (2003) A scalable video coding algorithm based DCTDWT, IEEE International. Signal Processing and Information Technology. pp. 247–249.
- [11] Paul P.J., and Girija, P.N. (2006) A novel VLSI architecture for image compression, Proceedings of ISM'06 Multimedia Eighth IEEE International. pp. 794–795.
- [12] Wahid, K.A., Islam, M.A., Shimu, S. S.M., Lee, H., and Ko, S. (2010) Hybrid architecture and VLSI implementation of the Cosine- Fourier-Haar

- transforms, Circuits, Systems, and Signal Processing, **29**(6): 1193–1205.
- [13] Jiang, S., and Hao, X. (2007) Hybrid Fourier-Wavelet image denoising, *Electronics Letters*, **43**(20): 1081–1082.
- [14] Ali, A.H. (2007) Combined DWT-DCT digital image water marking,” *Computer science*, **3**(9): 740–746.
- [15] Qi, H., Huang, Q., and Gao, W. (2010) A low-cost very large scale integration architecture for multistandard inverse transform, *IEEE Transactions on Circuits and Systems II: Express Briefs*, **57**(7): 551–555.
- [16] Fan C., and Su, G. (2009) Fast algorithm and low-cost hardware-sharing design of multiple integer transforms for VC-1, *IEEE Transactions on Circuits and Systems II: Express Briefs*, **56**(10): 788–792.
- [17] Fan, C. P., and Su, G.A. (2009) Efficient fast 1-d 8×8 inverse integer transform for VC-1 application, *IEEE Transactions on Circuits and Systems for Video Technology*, **19**(4): 1–7.
- [18] Wahid, K., Ko, S.B., and Teng, D. (2008) Efficient hardware implementation of an image compressor for wireless capsule endoscopy applications, *Proceedings of IEEE International Joint Conference Neural Networks*. pp. 2761–2765.
- [19] Shrestha, S., and Wahid, K. (2010) Hybrid DWT-DCT algorithm for biomedical image and video compression applications, *Proceedings of IEEE International Conference on Information Sciences, Signal Processing and Applications*. pp. 280–283.
- [20] Ghrare, S.E., Ali, M.A. M., Ismail, M., and Jumari, K. (2008) Diagnostic quality of compressed medical images: Objective and subjective evaluation, *Proceedings of Second Asia International Conference Modeling & Simulation AICMS 08*. pp. 923–927.
- [21] Hands, D.S., Huynh-Thu, Q., Rix, A. W., Davis, A.G., and Voelcker, R.M. (2004) Objective perceptual quality measurement of 3g video services, *IEEE International Conference of 3G Mobile Communication Technologies 3G*. pp. 437–441.
- [22] Wang, H.S.Z., Bovik A., and Simoncelli, E. (2004) Image quality assessment: From error measurement to structural similarity, *IEEE Trans. Image Processing*, **13**(4): 600–612.